npg

REVIEW

Energy transfer in plasmonic photocatalytic composites

Xiang-Chao Ma, Ying Dai, Lin Yu and Bai-Biao Huang

Among the many novel photocatalytic systems developed in very recent years, plasmonic photocatalytic composites possess great potential for use in applications and are one of the most intensively investigated photocatalytic systems owing to their high solar energy utilization efficiency. In these composites, the plasmonic nanoparticles (PNPs) efficiently absorb solar light through localized surface plasmon resonance and convert it into energetic electrons and holes in the nearby semiconductor. This energy transfer from PNPs to semiconductors plays a decisive role in the overall photocatalytic performance. Thus, the underlying physical mechanism is of great scientific and technological importance and is one of the hottest topics in the area of plasmonic photocatalysts. In this review, we examine the very recent advances in understanding the energy transfer process in plasmonic photocatalytic composites, describing both the theoretical basis of this process and experimental demonstrations. The factors that affect the energy transfer efficiencies and how to improve the efficiencies to yield better photocatalytic performance are also discussed. Furthermore, comparisons are made between the various energy transfer processes, emphasizing their limitations/benefits for efficient operation of plasmonic photocatalysts.

INTRODUCTION

Since the report on water splitting over titanium dioxide (TiO_2) by Fujishima *et al.*[1], semiconductor photocatalysts have received considerable attention in the field of solar energy conversion and utilization[2–4]. In conventional semiconductor photocatalysts, the semiconductor absorbs light by inter-band excitation of electrons, which generates electron–hole pairs. Then, the generated electrons and holes may be transferred to the surface of the semiconductor, where they initiate redox reactions. During the transfer process, the electrons and holes may also recombine with each other, which have no effect on the photocatalysis. Over the past 40 years, the main limitations of using semiconductor photocatalysts, such as TiO_2 and iron(III) oxide (Fe_2O_3), for large-scale applications have been the short-range light response, poor light absorption rate, and high recombination rate of photogenerated carriers, which result in low solar energy conversion efficiencies. Despite the considerable efforts to overcome these deficiencies, including extrinsic and intrinsic doping[5–10], sensitization[11–13], and surface treatment[14–17], significant breakthroughs have not yet been achieved.

In the recent efforts to develop photocatalytic materials, researchers tended to develop novel photocatalytic systems, such as the plasmonic photocatalyst[18,19], ferroelectric photocatalyst[20–23], and graphene-based photocatalyst[24,25], based on some basic physical principles. The plasmonic photocatalyst generally exhibits wide range and very efficient light absorption. Moreover, the exotic approach for generating electron–hole pairs often leads to a low carrier recombination rate. Thus, it has the greatest potential for improving many of the intrinsic

limitations of conventional semiconductor photocatalysts[13,26,27]. Following the development of the 'plasmonic photocatalyst' (Ag/SiO_2/TiO_2[18] and Ag/AgCl[19]) in 2008, it has received substantial interest, and many plasmonic photocatalysts have been developed[28–36]. For example, by depositing noble metal plasmonic nanoparticles (PNPs) onto conventional semiconductor photocatalysts (e.g., TiO_2, cadmium sulfide (CdS), and Fe_2O_3) in different ways[37–53], researchers have developed various plasmonic photocatalytic composites that exhibit significantly enhanced photocatalytic activities. In these composites, the PNPs efficiently absorb visible light through localized surface plasmon resonance (LSPR) and convert it into holes and electrons in the nearby semiconductors. Thanks to the intensive research over the past century, the physics about the LSPR of PNPs is well understood[54,55]. However, its role in plasmonic photocatalysts and particularly in the energy transfer from PNPs to semiconductors was mysterious when the system was developed. The LSPR-related energy transfer is an essential step in the plasmonic photocatalytic process, and it plays a vital role in determining the final photocatalytic performance. Therefore, the details of the energy transfer are of great scientific importance for understanding the excellent photocatalytic performance; technologically, they can also provide fundamental guidelines for optimizing the existing plasmonic systems and for developing new ones. Over the past several years, considerable experimental and theoretical efforts have been devoted to understanding this question and rapid progress is still being made.

There are many reviews in the literature on the applications and experimental preparation of plasmonic photocatalysts[27–34,56]. However, to the

School of Physics, State Key Laboratory of Crystal Materials, Shandong University, Jinan 250100, China
Correspondence: Y Dai, Email: daiy60@sdu.edu.cn

best of our knowledge, a systematic review on the energy transfer mechanism in plasmonic photocatalytic composites has not yet been published. This work is thus aimed at filling this gap. It begins with a brief introduction to the fundamental properties of the LSPR of PNPs, which is necessary to understand the energy transfer mechanism. Then, we present detailed discussions about the three energy transfer processes proposed thus far. These processes are the plasmon-induced hot electron injection, plasmon-induced resonance energy transfer, and plasmon-induced radiative energy transfer. In addition, in this review, we tentatively propose a new energy transfer process, called plasmon-induced direct electron injection. Finally, we end with a conclusion and an outlook on investigating the energy transfer processes for optimizing the plasmonic photocatalytic activity.

FUNDAMENTAL PROPERTIES OF LSPR

The LSPR of PNPs can include many plasmon modes, such as the dipole plasmon mode, quadrupole mode and considerably higher plasmon modes[55,57]. For photocatalytic applications, the most relevant mode is the dipole plasmon resonance. Therefore, in the present review, LSPR primarily refers to the dipole plasmon mode, which describes the collective oscillation of the conduction electrons in PNPs in response to the incident light. Upon light irradiation, the electric field will displace the conduction electrons relative to the nuclei, inducing a large electric dipole. Simultaneously, a restoring force arises because of the Coulomb attraction between electrons and nuclei, which results in resonant oscillation of the conduction electrons at a certain frequency. The LSPR generally occurs when the PNPs are considerably smaller than the wavelength of the incident light, as schematically illustrated in Figure 1.

The LSPR of PNPs can lead to very efficient absorption of light. For example, the absorption cross section of LSPR can be several or even tens of times greater than the physical cross section. As shown in Figure 1, LSPR can induce a large electric dipole, which oscillates at the same frequency as that of the electric field of the incident light[30,55]. This electric dipole can result in an intense electric field near the PNP, whose intensity can be tens to thousands of times greater than that of incident light[26,55,58]. This is the so-called near-field enhancement phenomenon. Because of the physical origin of near-field enhancement, it decays quickly when moving away from the PNP and is thus limited to the very vicinity of the PNP. As widely demonstrated, both the LSPR wavelength and absorption efficiency can be easily tuned by changing the sizes, shapes, compositions, and dielectric environments of PNPs[26,58–60]. Moreover, both the intensity and distribution range of
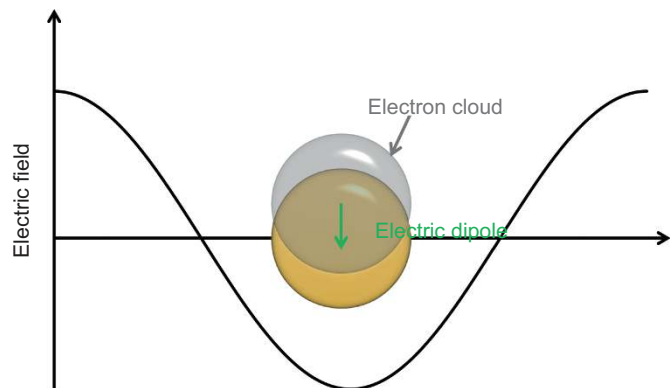
the near-field change accordingly. These properties of LSPR can lead to various energy transfer mechanisms from PNPs to semiconductors and provide versatile means for tuning the efficiency of each energy transfer process, which will be discussed in the following.

PLASMON-INDUCED HOT ELECTRON INJECTION FROM PLASMONIC METAL TO SEMICONDUCTOR

The generation of hot electrons in PNPs has been studied for several decades[27,34]. Here, the term 'hot electron' refers to electrons that are not in thermodynamic equilibrium with the atoms in a material. As introduced in the previous section, LSPR is characterized as the collective coherent oscillation of the conduction electrons in PNPs. Moreover, there exist two competitive ways for the dephasing of the resonant oscillation, namely, radiative emission of photons and non-radiative relaxation through electron–electron, electron–phonon, electron–surface, or electron–adsorbate scattering (Figure 2a, left)[59,61–64]. The hot electrons are generated during the non-radiative relaxation process primarily through electron–electron scattering, which results in intra- and inter-band excitation of the conduction electrons (Figure 2a, right). Note that the intra- and inter-band transition requires an energy overlap between the LSPR frequency and the transition energy. For Au, the threshold for the *d* to *s* inter-band transition is approximately 2.4 eV, which corresponds to a wavelength smaller than its LSPR wavelength at approximately 550 nm or longer
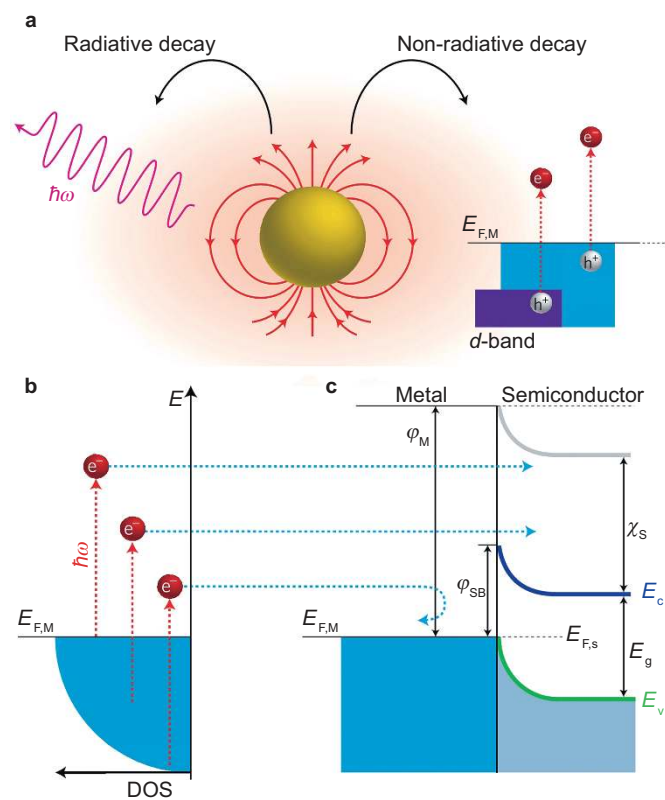

Figure 2 (**a**) LSPR can decay radiatively or non-radiatively. The radiative decay emits photons. During the non-radiative decay, hot electrons may be generated via intra- and inter-band excitation of the conduction electrons. (**b**) The energies of hot electrons have a wide distribution range. (**c**) The hot electrons with large energy can surmount the interface Schottky barrier, thus being injected into the conduction band of the semiconductor. Figure reproduced with permission: Ref. 27, © 2014 NPG. LSPR, localized surface plasmon resonance; DOS, density of states.

Figure 1 Schematic illustration of LSPR for a plasmonic nanosphere. LSPR, localized surface plasmon resonance.

wavelengths owing to the large dielectric constants of semiconductor substrates or special shapes of PNPs[26,53,65]. Consequently, the generation of hot electrons occurs primarily through the intra-band transitions in Au PNPs. In addition, the LSPR overlaps with intra-band excitations in Ag, which is also beneficial for generating reasonably high energy hot electrons. The energies of hot electrons have a wide distribution range (Figure 2b). It has been reported that the energies of hot electrons are approximately between 1 eV and 4 eV for Au and Ag PNPs[26,66]. Such energetic hot electrons may migrate to the adjacent semiconductor if their energies are larger than the Schottky barrier (SB) at the interface between the metal and semiconductor (Figure 2c). Moreover, although the energies of some hot electrons are not large enough to surmount the SB, they may also be injected into the semiconductor through the tunneling effect, as proposed by Mubeen *et al.*[67] As we can see, this hot electron injection mechanism is very similar to that of a dye-sensitized solar cell[13,68,69].

Recently, the Atwater and Louie groups theoretically investigated the generation of hot carriers from the decay of surface plasmon polaritons (SPPs) on metal-dielectric interfaces[70,71]. They noted that Au is beneficial for generating very hot holes rather than energetic hot electrons because of the special electronic structures. However, note that in their calculations, the energies of some modes of SPPs were large enough to excite the *d* to *s* inter-band transitions. This is often not true in the case of LSPR, whose energies are generally too small to initiate the inter-band transitions. Furthermore, the

geometry effect of confined PNPs on promoting intra-band transitions and thus forming hot electrons was also demonstrated by the Atwater group[70].

Experimentally, Zhao *et al.* first reported hints about plasmon-induced hot electron injection from Au/Ag to TiO$_2$[72]. When the incident light overlapped with the LSPR absorption of Au/Ag PNPs, they observed an increase in the anodic photocurrent for a TiO$_2$ film electrode containing dispersed Au/Ag PNPs. A breakthrough was achieved in 2003, when Ohko *et al.* reported the multicolor photochromism of a TiO$_2$ film containing Ag PNPs (Figure 3a), which provides strong evidence for the electron exchange between Ag and TiO$_2$ upon light irradiation[73]. Direct observation of the injection of hot electrons into the conduction band of TiO$_2$ was realized by Furube *et al.*[74] Because strong intra-band absorption in the infrared (IR) range can be observed when electrons are injected into the conduction band of TiO$_2$[75], they used femtosecond-resolved IR probing to detect any possible electron transfer from Au to TiO$_2$. Indeed, IR absorption was observed, and the ultrafast hot electron transfer from Au nanodots to TiO$_2$ was determined to be within 240 fs (Figure 3b and 3c). Subsequently, many experiments have also demonstrated the injection of hot electrons from PNPs to semiconductors, and different methods have been developed to probe the electron transfer[37,50,76–79]. For example, in a very recent study, using Ag$^+$ from AgNO$_3$ as electron probe ions and sodium citrate as a positive charge scavenger, Li *et al.* showed that Ag nanoparticles only form on the TiO$_2$ shell when the
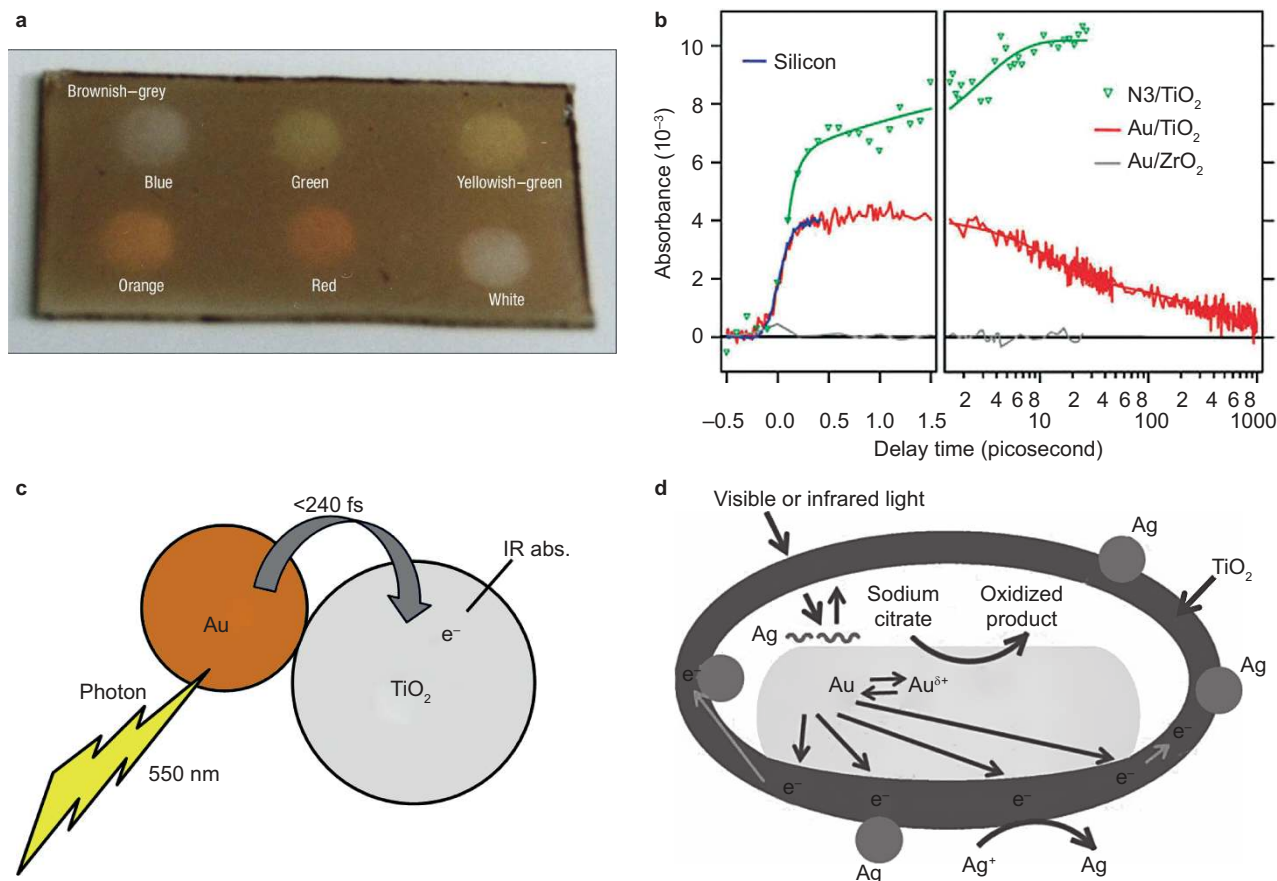
Figure 3 Experimental verifications of the hot electron injection energy transfer. (**a**) Photochromism of TiO$_2$ thin film dispersed with Ag PNPs, which originates from the electron exchange between Ag and TiO$_2$. (**b**) IR absorption of Au/TiO$_2$ in comparison with N3/TiO$_2$ and Au/ZrO$_2$. (**c**) Experimentally determined electron injection process and timescale. (**d**) Probe reaction of Ag$^+$, which is used to detect electrons. Figure reproduced with permission: a, Ref. 73, © 2003 NPG; b, c, Ref. 74, © 2007 ACS; d, Ref. 79, © 2015 Wiley-VCH. IR, infrared.

Au/TiO$_2$ is irradiated by light with the LSPR wavelength of Au, which confirms the injection of hot electrons from Au to TiO$_2$ (Figure 3d)[79].

As shown in Figure 2c, when a metal is brought into contact with an *n*-type semiconductor, an interface SB is formed. For a high rate of hot electron injection, the energies of the hot electrons must surpass the barrier. Considerable efforts are thus expended to theoretically study this dynamic process. For Au/TiO$_2$, a moderate SB of approximately 1 eV is formed according to the Schottky–Mott theory[30,80]. Because the energies of hot electrons typically range between 1 eV and 4 eV above the Fermi level, the small SB makes efficient electron transfer from Au to TiO$_2$ energetically possible, which also renders Au/TiO$_2$ a model system for studying and utilizing the hot electron injection process. Due to the suitable band alignments, hot electron injection has also been observed in many other PNP-sensitized semiconductors, such as Ag/TiO$_2$, Au/ZnO, Au/WO$_3$, and Au/CdS (Figure 4a)[37,50,78,81]. However, a small SB does not necessarily ensure hot electron transfer. For example, hot electron transfer has never been experimentally observed in Au/Fe$_2$O$_3$, although the SB of Au/Fe$_2$O$_3$ is considerably smaller than that of Au/TiO$_2$[82]. This result indicates that some unknown factors may also determine the hot electron transfer in addition to the SB. In a recent theoretical study, Long *et al.* showed that effective hybridization of the unoccupied states in the metal and semiconductor is very important for efficient injection of hot electrons from the metal to semiconductor (Figure 4b and 4c)[52].

The solar utilization efficiency through the hot electron injection is generally very low. For example, Mubeen *et al.* elaborately devised an autonomous plasmonic solar water splitter that consisted of gold nanorods and a crystalline TiO$_2$ layer, in which all of the electrons and holes originate from the hot electron injection energy transfer (Figure 5a)[51]. They showed that the solar to energy conversion efficiency is only approximately 0.1%. For practical applications, this conversion efficiency should be enhanced much further. Based on the mechanism of hot electron injection, there are two important factors that can affect the solar utilization efficiency, namely, the hot electron generation efficiency (HEGE) and the hot electron injection efficiency (HEIE). Here, HEGE refers to the efficiency of converting LSPR into energetic hot electrons moving to the semiconductor. In some samples, the PNPs are relatively large (e.g., larger than 40 nm),

which leads to a low HEGE primarily due to the prominent scattering effect. Although the generation of hot electrons from the decay of LSPR is very efficient in small PNPs, the portion of hot electrons moving toward the semiconductor is still low provided that the momentum-direction distribution of hot electrons is approximately isotropic and that the PNPs are generally atop the semiconductor.

Over the past few years, researchers have found a number of ways to improve the HEGE. Giugni *et al.* showed that the HEGE can be significantly increased through adiabatic compression of SPPs in a nano-cone of Au[83]. This is because the special structure can efficiently transform the propagating wave of SPPs into a quasi-static local field and then into hot electrons moving to the semiconductor (Figure 5b). In fact, combining SPPs with a semiconductor photocatalyst can provide other means for enhancing the photocatalysis. For example, by elaborately designing a hybrid structure of Au/Fe$_2$O$_3$, Li *et al.* showed that the SPPs can significantly enhance the photocatalysis through confining the light in Fe$_2$O$_3$ and thus increasing its light absorption efficiency[84]. In a photodetection device composed of Au/Si, Knight *et al.* showed that a photocurrent maximum is generated at the LSPR peak wavelength (Figure 5c)[85]. This suggests that the HEGE is enhanced when the LSPR absorption efficiency increases. The surrounding medium also plays an important role in the HEGE. It was shown that the 1 nm Ti metal interface between Au and Si is responsible for producing 33% of the hot electrons, which can increase to more than 50% for a thickness of 5 nm[85].

For a specific plasmonic system, the composite structure also affects the HEGE. As shown in Figure 6a, upper, when the PNP is atop a semiconductor, only the hot electrons with momentum falling within the small red shaded cone in the momentum space may be injected into the semiconductor. This can be significantly improved if one embeds the PNP into the semiconductor to some extent, as show in Figure 6a, lower. Then, the hot electrons with momentum falling within the large red-shaded cone may be injected into the semiconductor. Therefore, considerably higher photocatalytic activities have been reported for the partially or fully embedded plasmonic photocatalytic systems[43,67,79,86–88]. It has recently been proposed that the Janus structure may promote the generation of hot electrons with momentum mainly pointing toward the semiconductor, thus also
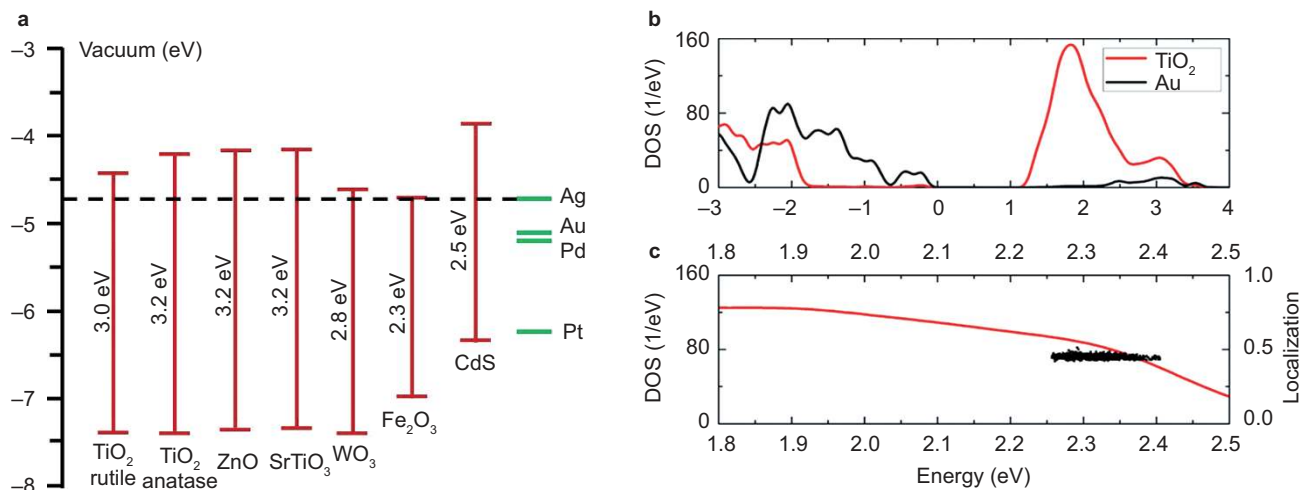

Figure 4 (**a**) Energy band positions of some common semiconductor photocatalysts and plasmonic metals. The energies are given on a potential scale vs. vacuum. (**b**) The theoretically computed density of states (DOS) of a Au/TiO$_2$ system. (**c**) The DOS of TiO$_2$ (red line) in the excitation energy range and the localization of LSPR excitation on the simulated Au$_{20}$ cluster (black squares), which show the strong hybridization of the excitation states in TiO$_2$ and Au. Figure reproduced with permission: b, c, Ref. 52, © 2014 ACS.
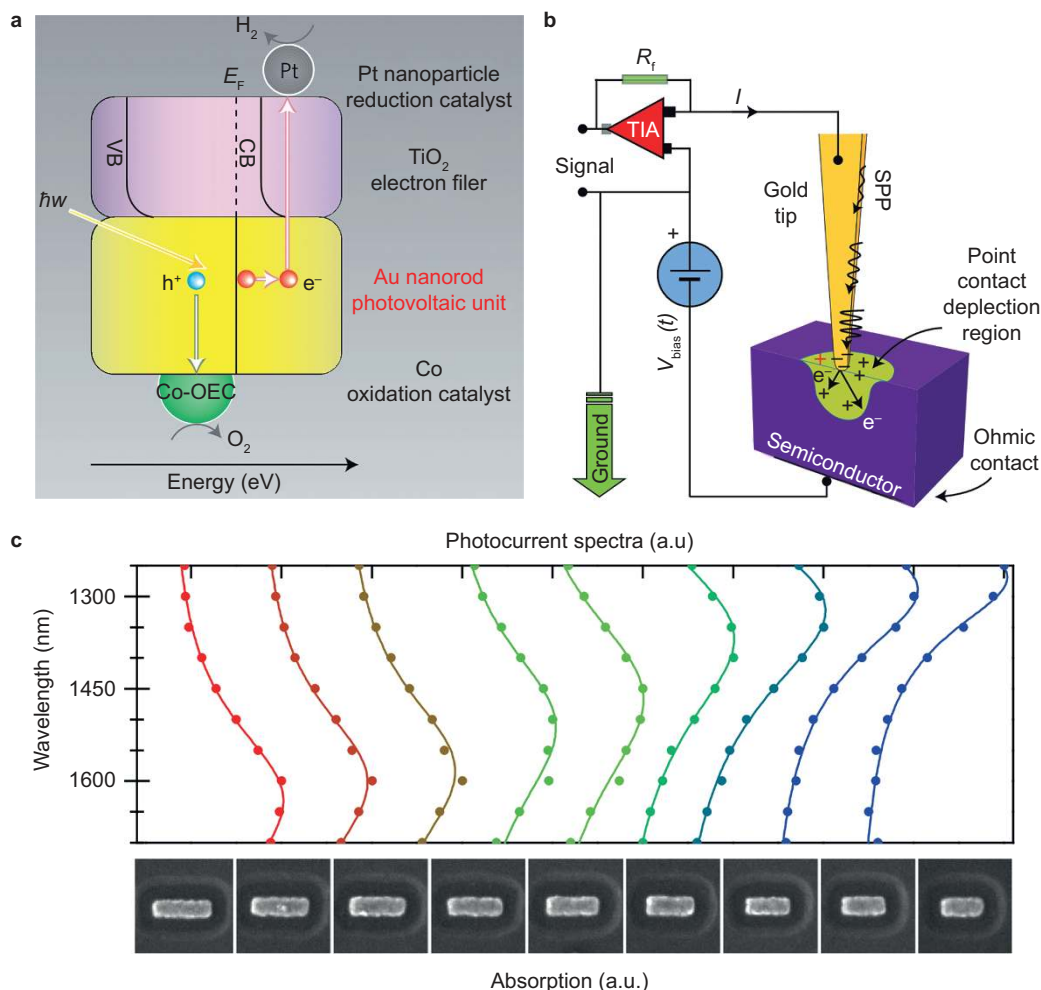
Figure 5 (**a**) Energy level diagram showing the generation and transfer of carriers in the plasmonic solar water splitter devised by Mubeen *et al*. (**b**) Schematic of the setup devised by Giugni *et al*. (**c**) Photocurrent spectra for a specific Au antenna, which is consistent with the calculated absorption spectra due to LSPR. Figure reproduced with permission: a, Ref. 51, © 2013 NPG; b, Ref. 83, © 2013 NPG; c, Ref. 85, © 2011 AAAS. LSPR, localized surface plasmon resonance; SPP, surface plasmon polariton.

increasing the HEGE[48,89,90,91]. In addition, for a free-electron metal, the momentum-direction of generated hot electrons should mainly be along the oscillation direction of LSPR according to momentum conservation. Therefore, any structures that facilitate oscillation of LSPR along the interface normal to the metal-semiconductor composite will primarily generate hot electrons that move to the semiconductor and thus increase the HEGE.

Theoretically, the HEIE is generally described by a modified Fowler equation[83,86], which indicates that the HEIE decreases with increasing SB or with decreasing hot electron energy relative to the SB. For example, because the conduction bands of ZrO_2/SiO_2 lie much higher in energy than that of TiO_2, which results in a larger interface SB in Au/ZrO_2 and Au/SiO_2, there is essentially no hot electron injection in these systems[74,85]. Li *et al*. also recently demonstrated the effect of hot electron energy relative to the SB on the HEIE by comparing the hot electron transfer properties in Au-TiO_2 and CdS-Au-TiO_2[92]. For a specific metal-semiconductor system, the interface SB depends strongly on the interfacial chemical and electronic structures[91,93–95]. This provides plenty of room to optimize the interface SB for improving HEIE. For instance, Tamura *et al*. recently demonstrated that the interface SB of Pt/TiO_2 is strongly affected by the interface oxygen

deficiency[95]. They showed that the interface contact type can be changed from a Schottky- to Ohmic-type contact by varying the interface oxygen deficiency (Figure 6b). Our group also demonstrated that the replacement of O by Au atoms at the Au/TiO_2 interface can increase the interface SB (Figure 6c)[91]. In addition, because hot electrons lose energy very quickly through electron–electron or electron–phonon scattering, it is better to achieve ultrafast hot electron extraction for improving the HEIE. This factor has been highlighted in recent reviews[27,34,96]. Thus, we do not discuss it in detail.

Although the hot electron injection energy transfer process can generate electron–hole pairs using visible or even IR light, which increases the solar energy utilization, there are many limitations on this energy transfer process for photocatalytic applications. As shown above, this energy transfer process requires proper band alignments and efficient electronic coupling between PNPs and the semiconductor to ensure an efficient HEIE. Thus, direct contact between PNPs and the semiconductor is required. Consequently, some plasmonic metals such as Ag and Cu, which are easily degraded, are not applicable for supporting this energy transfer process. Moreover, upon the injection of hot electrons, a large amount of hot holes are left in the PNPs. These holes must be immediately compensated to retain a
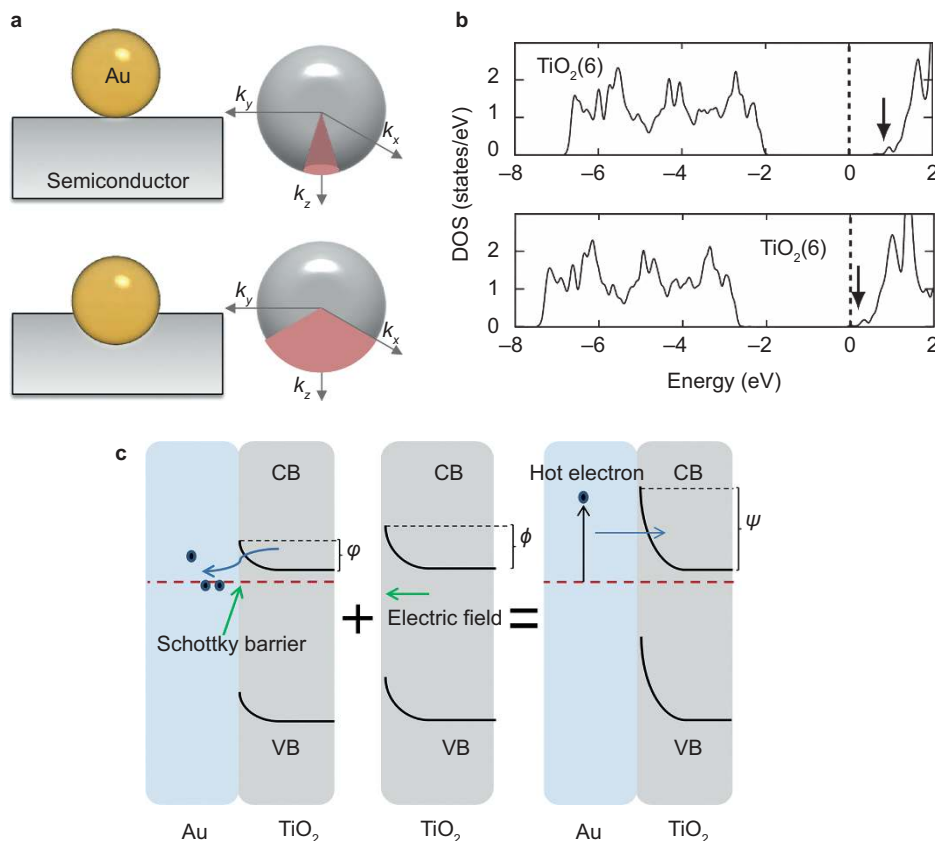
Figure 6 (**a**) The hot electrons can transport only through the small bottom interface when the PNP is atop the semiconductor (upper); the interface area through which the hot electrons can transfer into the semiconductor is significantly increased when the PNP is partially embedded into the semiconductor (lower). (**b**) The Fermi levels relative to the conduction band of TiO$_2$ for stoichiometric (upper) and fully reduced (lower) Pt/TiO$_2$ interfaces. (**c**) The band bending induced by replacing O with Au atoms at the interface, which further increases the interface SB. Figure reproduced with permission: b, Ref. 95, © 2009 APS; c, Ref. 91, © 2014 ACS.

sustainable LSPR. Therefore, an electron donor or hole-transporting material should be in contact with the PNPs. This is the so-called charge balance requirement[27]. These requirements of band alignment, electronic coupling and charge balance can impose strict limitations on the selection of materials for preparing efficient plasmonic photocatalysts. In addition, to prevent the injected hot electrons from flowing readily back into the PNPs, upward band bending in the semiconductor is required (Figure 2c). This means that only *n*-type semiconductors are preferred. Very recently, Lin *et al.* demonstrated that under UV-Vis light irradiation, the injection of hot electrons from Au to TiO$_2$ shortens the lifetime of electrons generated upon UV light irradiation in TiO$_2$[97]. This result indicates that the hot electron injection may also have a negative effect on the intrinsic photocatalytic activity of conventional photocatalysts.

PLASMON-INDUCED DIRECT ELECTRON INJECTION FROM PLASMONIC METAL TO SEMICONDUCTOR

When the dimension of PNPs is comparable to or smaller than the electronic mean free path and there are adsorbates on the PNPs, another ultrafast dephasing channel for LSPR, known as chemical interface damping, may dominate. In this dephasing channel, the interaction of LSPR with adsorbates induces dephasing through the direct excitation of resonant electrons into the unoccupied states of adsorbates[98,99]. Note that in this process, energy conservation has to be satisfied, that is, the energy of the unoccupied states of adsorbates relative to the Fermi level of the plasmonic metal must overlap with the LSPR energy. This direct electron

injection to adsorbates has been widely demonstrated in atoms or small molecules adsorbed PNP systems[100–102], for which an excellent review by Christopher *et al.* was recently published[103]. Similarly, it is highly expected that this mechanism also exists in plasmonic photocatalytic composites. Experientially, it has been suggested to exist in Ag/SiO$_2$[99].

Compared with the hot electron injection mechanism, this is a potentially more efficient mechanism that overcomes the momentum, energy, and time scale requirements of hot electron transfer. However, for this energy transfer mechanism to efficiently contribute to the photocatalytic activity of plasmonic metal-semiconductor composites, the interfacial unoccupied states to which the resonant electrons are excited must lie higher in energy than the conduction band of the semiconductor far from the interface to facilitate the transfer of injected electrons out of the interfacial region where they cannot initiate redox reactions (see Figure 7). At present, the interfacial electronic structures between PNPs and semiconductors are poorly understood. There are also few experimental reports in the literature about this plasmon-induced direct electron injection. Therefore, if and how this direct electron injection mechanism functions in the plasmonic composite require further studies in the future.

PLASMON-INDUCED RESONANCE ENERGY TRANSFER

Among researchers studying plasmonic photocatalysts, two different terms are generally used to refer to the plasmon-induced resonance energy transfer. Here, we discuss them separately.
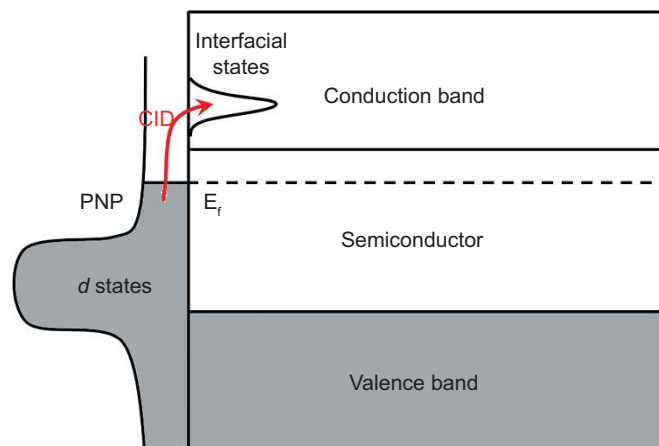
Figure 7 Schematic illustration of direct electron injection from a PNP to a semiconductor via CID. PNP, plasmonic nanoparticle; CID, chemical interface damping.

ENERGY TRANSFER THROUGH NEAR-FIELD ENHANCEMENT

The optical absorption mechanism of a semiconductor is generally described by Fermi's golden rule in the electric dipole approximation as follows[58,104]:

$$w_{k \to m}^0 = (2\pi e^2/\hbar) E_0^2 |p_{mk}|^2 \delta(E_m - E_k - \hbar\omega)$$

where E_0^2 is the intensity of the electric field of incident light, $|p_{mk}|$ is the momentum matrix element in the semiconductor, and E_k and E_m are the energies of the initial and final states in the electron transition, respectively. As shown, the absorbance increases linearly with the intensity of the perturbation electric field. In the section 'Fundamental Properties of LSPR', we indicated that the plasmonic dipole can induce near-field enhancement. Electromagnetic simulations using the finite-difference time-domain (FDTD) or discrete dipole approximation (DDA) method revealed that the intensity of the plasmon-induced near-field can reach tens to thousands of times that of the incident light[26,55,58]. Thus, the near-field can significantly enhance the inter-band or other optical transitions in the nearby semiconductor if the LSPR spectra overlap with them. The full enhancement (FE) of light absorption can be estimated using the following equation:

$$FE = \frac{\int_V dz \int dxdy |E(x, y, z)|^2}{\int_V dz \int dxdy |E_0|^2}$$

where the integrating volume V refers to the volume in the semiconductor covered by the near-field. $E(x,y,z)$ is the value of the near-field at point (x,y,z), and E_0 is the electric field of incident light. This energy transfer through near-field enhancement is easy to understand and has been widely demonstrated experimentally[18,45,46,58,65], for which some exhaustive reviews are available[26,32,96]. Here, we do not discuss them in detail.

ENERGY TRANSFER THROUGH DIPOLE–DIPOLE COUPLING

Another term for the plasmonic resonance energy transfer was proposed by Cushing *et al.* in 2012[104]. From their perspective, the plasmonic resonance excites electron–hole pairs in the semiconductor by coupling of the large plasmonic dipole to the electron–hole pair dipole in the semiconductor. This picture is very similar to the F—rster resonance energy transfer, in which the fluorescent donor is replaced

by the plasmonic dipole[105]. In their original work, core-shell Au@Cu₂O and sandwiched Au@SiO₂@Cu₂O particles were elaborately prepared to isolate the various plasmonic energy transfer processes. Because of the insertion of an insulating silica layer in Au@SiO₂@Cu₂O, the related electron injection energy transfer is ruled out. As shown in Figure 8a and 8b, the photocatalytic action spectra of Au@Cu₂O and Au@SiO₂@Cu₂O follow the trend of the extinction spectra of the corresponding systems. Thus, the involvement of LSPR in creating electron–hole pairs is verified. Moreover, the results of transient-absorption spectroscopy show that the number of carriers generated in Cu₂O obeys the dipole–dipole interaction rules (Figure 8c and 8d). Therefore, they proposed that the energy transfer occurs through dipole–dipole coupling.

This energy transfer mechanism is based on the following physics. As introduced above, the interaction of the semiconductor with an electromagnetic field is described in the electric dipole approximation. From the semi-classical perturbation theory, the interaction Hamiltonian between a dipole $\vec{\mu}$ and electric field $\vec{E}$ can be expressed as $H' = -\vec{\mu} \bullet \vec{E}$[106]. Replacing $\vec{E}$ with the electric field induced by the plasmonic dipole, the perturbation Hamiltonian H' becomes the dipole–dipole interaction term $H_{AB} = \frac{\mu_A \mu_B}{r^3}(3(\hat{\mu}_A \bullet \hat{r})(\hat{\mu}_B \bullet \hat{r}) - (\hat{\mu}_A \bullet \hat{\mu}_B))$, where μ_A and μ_B refer to the plasmonic and electron–hole pair dipoles, respectively. Then, one can obtain the transition probability using Fermi's golden rule:

$$w_{AB} = \frac{2\pi}{\hbar^2} |H_{AB}|^2 (\delta(E_A - E_B - \hbar\omega) + \delta(E_A - E_B + \hbar\omega))$$

Based on some approximations and simplification, Cushing *et al.* showed that the full enhancement in the light absorption of a semiconductor can be approximately 10 000 for their Au@Cu₂O samples. This large increase in light absorption can significantly enhance the solar utilization efficiency. Since this mechanism was proposed, it has been widely used to explain experimentally obtained results[29,40,47,49,107,108].

As can be seen, the two viewpoints are identical and are based on the same physical principle that the plasmonic dipole is coupled with the electron–hole pair dipole in the semiconductor through the near field it induced. In the first viewpoint, the near field induced by the plasmonic dipole is often explicitly calculated using the FDTD or DDA method. In contrast, in the second viewpoint, the near field is implicitly expressed by a formula.

Based on the plasmon-induced resonance energy transfer mechanism, there are three important factors that can affect the energy transfer efficiency: the overlap between LSPR absorption and optical transitions in the semiconductor, the intensity of the enhanced near-field and the volume in the nearby semiconductor that the enhanced near-field can cover. Generally, the optical transition of a semiconductor can be tuned by selective doping with intrinsic or extrinsic dopants, which has been widely studied and reviewed over the past decades[5–9]. Here, we focus mainly on tuning the properties related to LSPR. Both experimental and theoretical results have shown that the three factors are generally correlated with each other[55,58,60]. Using Ag@AgCl as a model system, we showed that the LSPR absorption can be easily tuned to cover the entire visible light range by varying the size, shape, and dielectric environment of Ag PNPs (Figure 9). Moreover, both the intensity and distribution range of the enhanced near-field change accordingly[58]. In Figure 10, the characteristics of the near-field around Ag nanorods with different aspect ratios are shown. Overall, both the intensity and distribution range of the near-field increase with the LSPR absorption efficiency. In addition, compared with the transverse mode, the longitudinal plasmon mode of silver nanorods is more effective in extending LSPR absorption and increasing the intensity and distribution range of the near
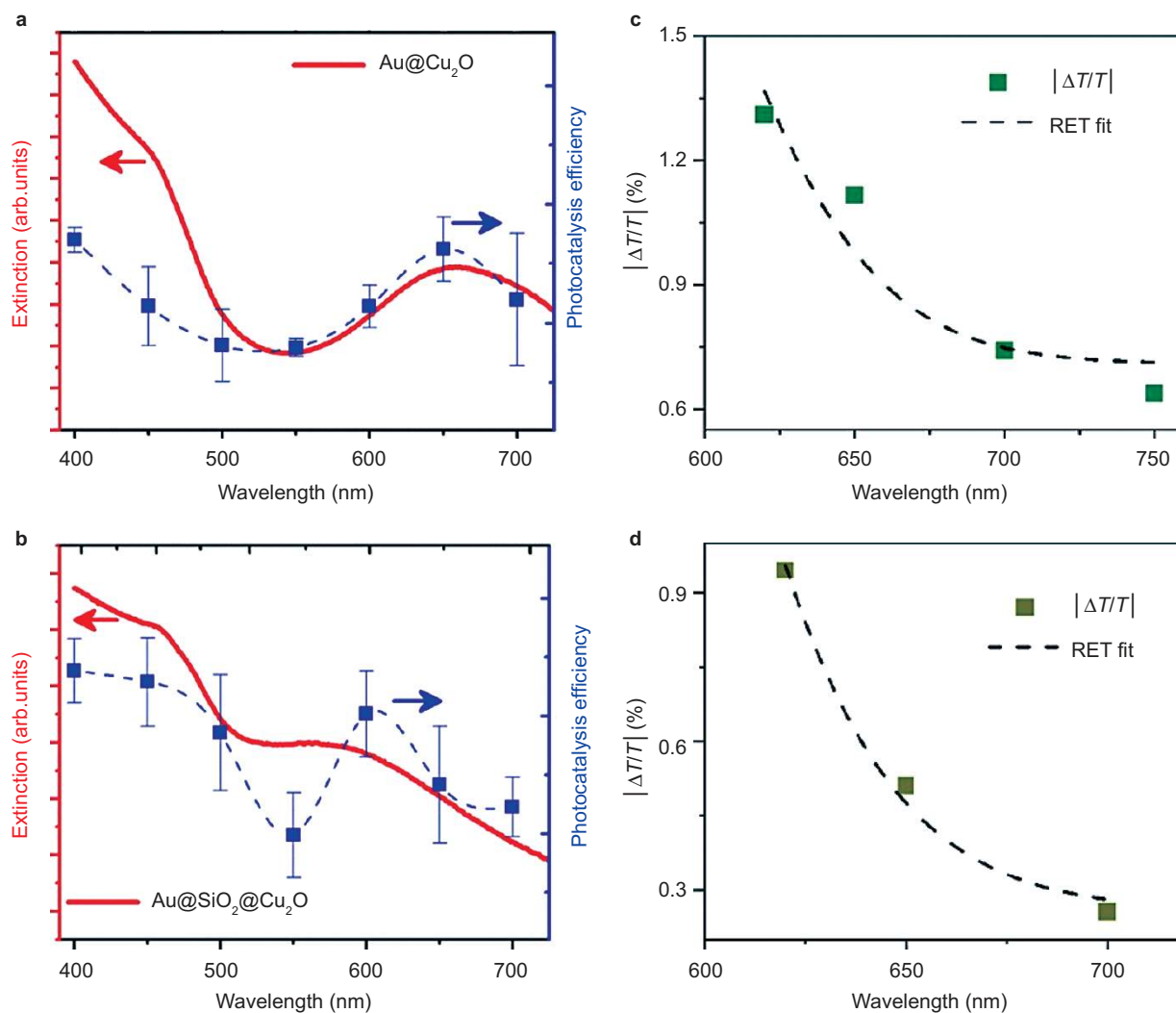
Figure 8 The extinction spectra and photocatalytic action spectra for Au@Cu$_2$O (**a**) and Au@SiO$_2$@Cu$_2$O (**b**). (**c**) and (**d**) show the wavelength-dependent signal amplitudes (which measure the carrier density) for Au@Cu$_2$O and Au@SiO$_2$@Cu$_2$O, respectively; each result is also fit with the plasmon-induced resonance energy transfer (RET) model on the basis of dipole–dipole interaction rules. Figure reproduced with permission: Ref. 104, © 2012 ACS.

field. In a recent study, Near *et al.* showed that there is a modified linear relationship between the wavelength of the longitudinal LSPR mode and the aspect ratio of Au nanorods. Moreover, the relationship between the Au nanorod diameter and extinction intensity is linear within a specific aspect ratio[109]. Similar linear relationships are also found for Ag nanorods[110]. These results can allow for the facile determination of the dimensions of nanorods necessary to generate the desired LSPR characteristics.

Given the benefits of Au nanorods in this energy transfer process, Liu *et al.* experimentally prepared gold-nanorod-photosensitized TiO$_2$[53]. They showed that broadband visible light absorption can be easily realized by varying the aspect ratio of Au nanorods. Moreover, the enhancement of activity induced by the longitudinal plasmon mode is indeed larger than that induced by the transverse mode. Li *et al.* recently reported the preparation of Au nanorod@TiO$_2$ yolk-shell nanostructures[79]. Significantly enhanced photocatalytic activity was obtained. Given the ability to convert low energy light at a specific wavelength by tuning the aspect ratio of Au nanorods, they proposed the potential for designing photocatalysts with specific light harvesting. In addition, many other Au/Ag nanorod-sensitized semiconductor photocatalysts have also been reported with enhanced photocatalytic performance[39,87,88,111,112].

The benefits of plasmon-induced resonance energy transfer for improving the photocatalytic activities of traditional semiconductor photocatalysts include the following: (i) increasing the rate of electron–hole formation in the regions of semiconductor covered by the near field, and (ii) localizing the generation of electron–hole pairs mostly near the surface of semiconductor; therefore, the recombination during their migration can be significantly decreased. The benefit of (ii) is particularly important for materials that suffer from severe bulk recombination of carriers, such as Fe$_2$O$_3$. It has been demonstrated that Au/Fe$_2$O$_3$ exhibits significantly enhanced solar to fuel energy conversion efficiency[46]. Additionally, in comparison with the hot electron injection energy transfer, this energy transfer is not constrained by the requirements of band alignment, electronic coupling and charge balance, thus offering more flexibility in the selection of materials for photocatalytic applications.

PLASMON-INDUCED RADIATIVE ENERGY TRANSFER

As introduced above, the LSPR of PNPs can also decay radiatively. The emitted photons may be absorbed by the nearby semiconductor, generating electron–hole pairs, if their energies are large enough. This
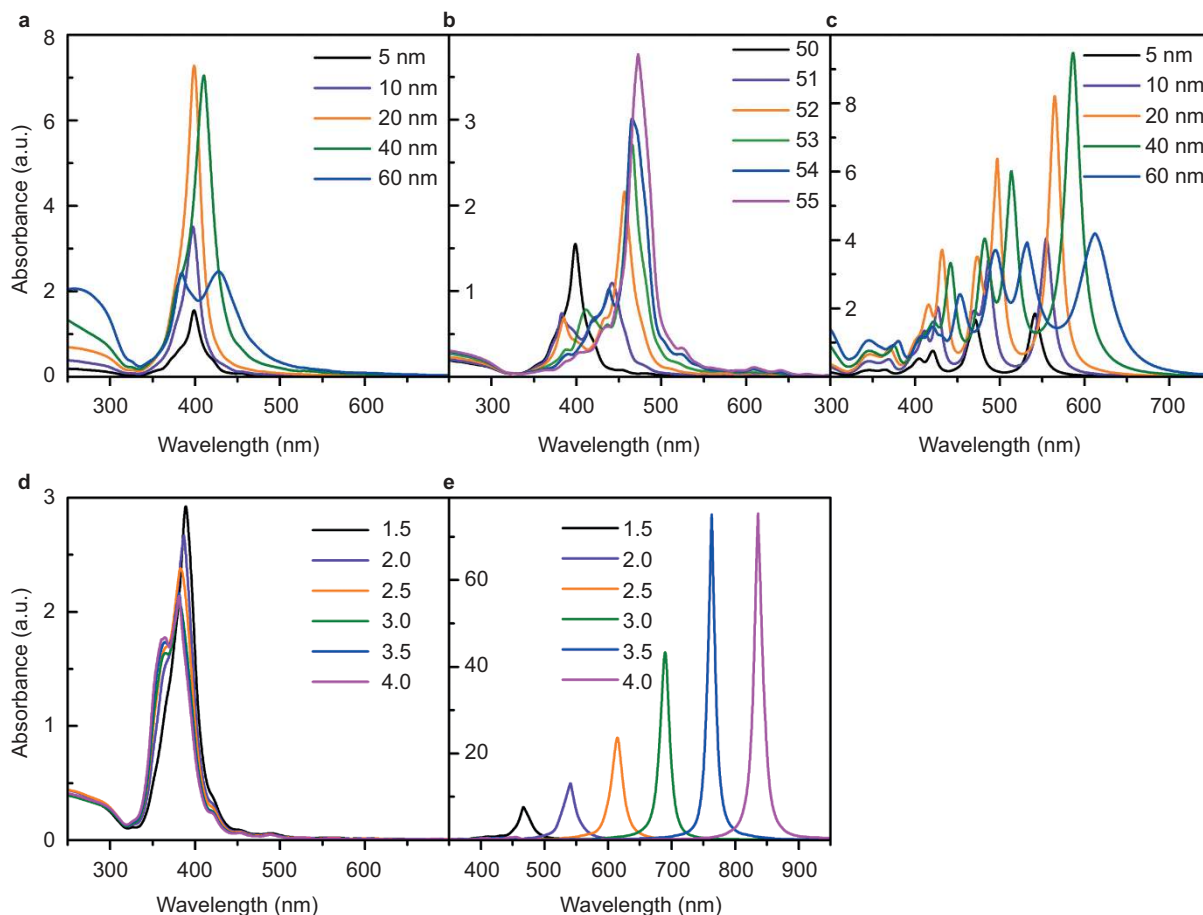
Figure 9 The LSPR absorption efficiencies and wavelengths of different Ag PNPs on AgCl. (**a**) Ag nanospheres with different diameters. (**b**) A Ag nanosphere (diameter of 5 nm) embedded in AgCl at different depths. (**c**) Ag nanocubes with different edge lengths. (**d**) and (**e**) are for the transverse and longitudinal modes of silver nanorods with different aspect ratios, respectively. Figure reproduced with permission: Ref. 58, © 2014 ACS.

energy transfer process was indirectly demonstrated by Kumar *et al*.[113] They observed that when the SiO_2 layer between Ag and TiO_2 is thick enough that the other plasmonic enhancement effects are well ruled out, the photocatalytic activity is still enhanced. The only explanation is thus the plasmon-induced radiative energy transfer. At the early stage of development of plasmonic photocatalysts, this energy transfer mechanism was proposed to explain the experimental results[26,42,114]. However, an increasing number of studies have shown that the contribution of this energy transfer process is very limited. In particular, the radiative efficiency is very low when the PNPs are small[57,115,116]. Dulkeith *et al*.[116] showed that the luminescence quantum yield of Au nanospheres in the range of 2–35 nm is only on the order of 10^{-6}. Because plasmonic metal interacts with the semiconductor through the electromagnetic field it induced, Cushing *et al*. used a full quantum electrodynamics theory to treat this interaction process and concluded that the radiative contribution is virtually negligible[104].

In contrast, the radiative decay typically dominates in large PNPs. For example, when the size of Ag PNPs exceeds 40 nm, the radiative decay becomes dominant[57]. Nevertheless, it has been shown that the radiative energy transfer contributes only less than 25% to the enhancement of the photocatalytic performance[30,113,117]. This is probably because the structures of the plasmonic composites are generally irregular, which cannot effectively utilize the scattering effect. In the field of photovoltaics, however, it has been widely demonstrated that

the prominent scattering effect of relatively large PNPs can efficiently trap light in the semiconductor layer in elaborately designed solar cells[118], as schematically shown in Figure 11. This light trapping can significantly increase the effective optical path length in the semiconductor and thus the light absorption efficiency. Similarly, one may potentially obtain the best radiative energy transfer in plasmonic photocatalysis by optimizing the hybrid structures of plasmonic photocatalysts. This may be more easily realized in the photoelectrode of photoelectrochemical cells because of the relatively easy control of the microstructures.

CONCLUSION AND OUTLOOK

The unique energy transfer from PNPs to conventional semiconductor photocatalysts is one of the most prominent characteristics of plasmonic photocatalysts. This specialty has established a new paradigm in the harvesting of solar energy for photocatalytic applications. This work reviews and discusses the three energy transfer processes proposed in previous studies. In general, the primary energy transfer processes are plasmon-induced hot electron injection and resonance energy transfer, while plasmon-induced radiative energy transfer is very limited at present. The specific structure of the plasmonic photocatalytic composite can affect both the generation and injection efficiencies of hot electrons, thus determining the energy transfer efficiency based on the plasmon-induced hot electron injection
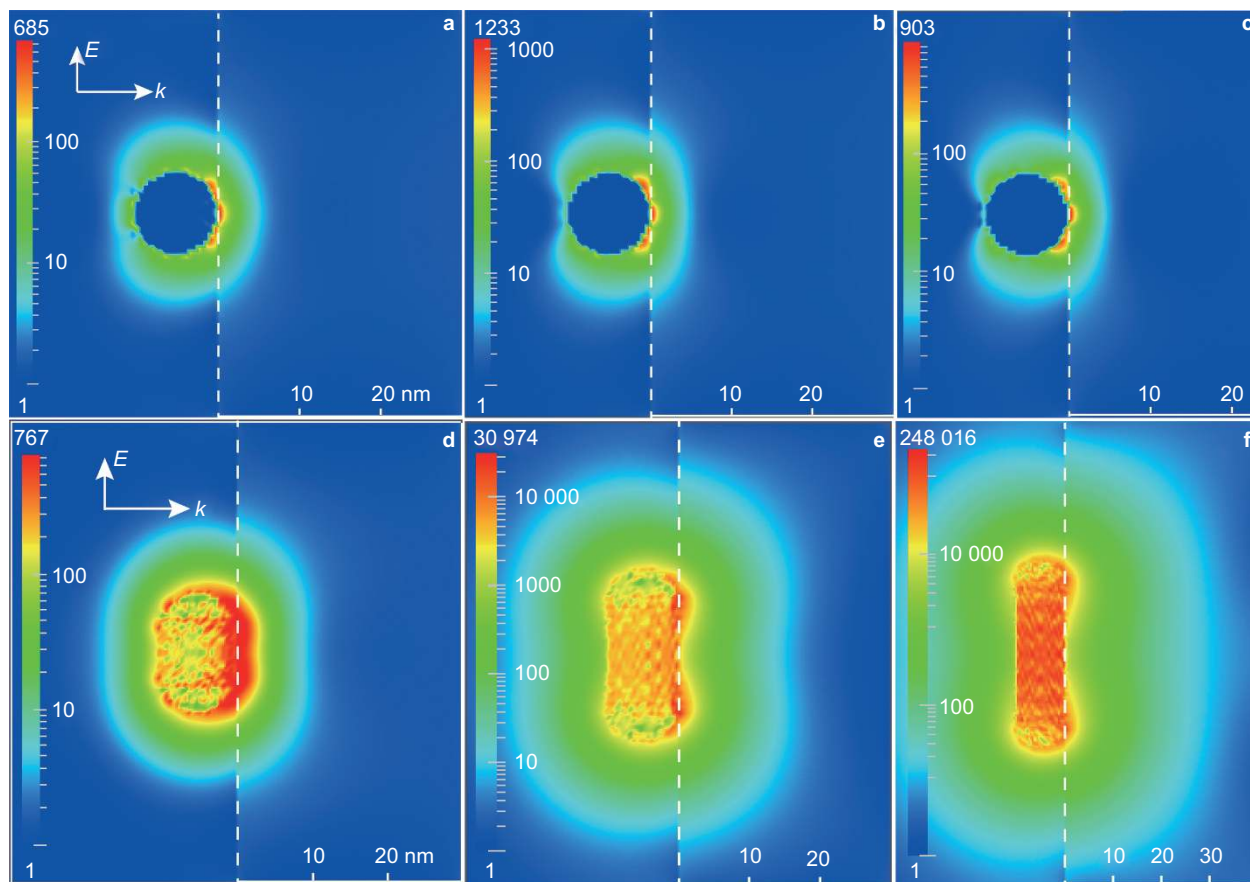
Figure 10 The near-field enhancements (given by $|E|^2/|E_0|^2$) induced by the transverse LSPR-mode of a Ag nanorod with aspect ratios of (**a**) 1.5, (**b**) 2.5, and (**c**) 4.0. (**d**), (**e**) and (**f**) respectively show the corresponding results induced by the longitudinal mode. The depicted cross sections bisect the corresponding Ag nanorods. Figure reproduced with permission: Ref. 58, © 2014 ACS.

process. The plasmon-induced resonance energy transfer depends on the near-field enhancement and the overlap between the LSPR absorption and the optical transitions in semiconductors. In addition, this
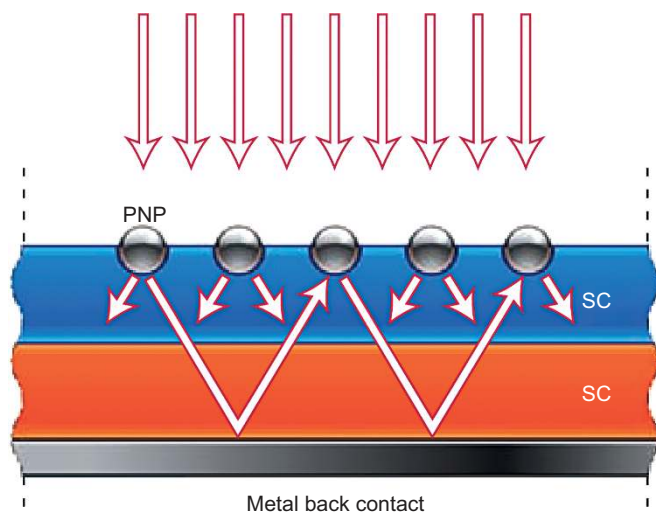

Figure 11 Light trapping in a semiconductor by combining the scattering from PNPs at the surface of a solar cell with reflecting from a metal back contact. Figure adapted with permission: Ref. 118, © 2010 NPG. PNP, plasmonic nanoparticle; SC, semiconductor.

energy transfer process localizes the generation of electron–hole pairs mainly near the PNPs, which significantly decreases the carrier recombination rate. On the other hand, for the hot electron injection process to occur, many requirements, such as proper band alignment and electronic coupling between the metal and semiconductor and charge balance during photocatalysis, should be satisfied. This imposes strict limitations on the selection of materials for preparing efficient plasmonic photocatalysts. In contrast, the plasmon-induced resonance energy transfer is not constrained by such requirements. With a better understanding of the energy transfer mechanisms, considerably more efficient plasmonic photocatalytic systems may be intentionally devised, which would ultimately enable the industrialization and commercialization of photocatalytic technology.

As a relatively new and burgeoning filed, one can anticipate that new understanding of the physical processes underlying the energy transfer processes will be achieved and that new energy transfer processes may also be proposed. Here, we present an outlook on their development in the near future:

(1) For hot electron injection energy transfer, many factors that affect the generation of hot electrons have been experimentally revealed, including the size, shape, and dielectric environment of PNPs. However, the underlying physics is not well understood. Recently, Govorov *et al.* developed a series of theories for the dynamic response of typical plasmonic NPs, which can be used to study the generation of hot electrons[119–122]. It is expected that

the widespread applications of these theories will not only provide a deeper understanding of the factors that affect the generation of hot electrons but also reveal new ones. Additionally, the interface SB is often estimated in the Schottky–Mott limit, which is generally too simple to provide the correct band alignment between the metal and semiconductor. Moreover, the interface chemical and electronic structures often affect the interface SB. Therefore, systemic investigations of the band alignments between plasmonic metals and semiconductors are expected for understanding and optimizing the relevant experimental results. In this respect, first principle studies may contribute substantial information[91,93–95].

(2) Here, we tentatively propose the potential of direct electron injection from PNPs to semiconductors. However, the detailed interfacial electronic structures require further study to confirm whether this can be an effective energy transfer process in plasmonic photocatalytic composites.

(3) For plasmon-induced resonance energy transfer, there are still different viewpoints. For example, Zhang et al. named this plasmon-induced resonance energy transfer the LSPR-powered bandgap breaking effect[30]. In their picture, the electron collisions at the metal-semiconductor interface excite electrons from the valence band of the semiconductor to the conduction band, thus generating electron–hole pairs. In our opinion, this way of generating electron–hole pairs may indeed occur at the interface, which arises from the non-radiative decay of LSPR and does not contradict the plasmon-induced resonance energy transfer. Instead, it may be regarded as a new energy transfer process. Furthermore, this energy transfer may occur only if the plasmonic metal and semiconductor are in direct contact. In many reports in the literature, the plasmon-induced resonance energy transfer is often also regarded as the near-field enhancement mechanism. This generally confuses new researchers in this field. When reviewing the literature, it is important to note that they are actually identical.

COMPETING INTERESTS
The authors declare no competing financial interests.

1 Fujishima A, Honda K. Electrochemical photolysis of water at a semiconductor electrode. *Nature* 1972; **238**: 37–38.

2 Chen XB, Shen SH, Guo LJ, Mao SS. Semiconductor-based photocatalytic hydrogen generation. *Chem Rev* 2010; **110**: 6503–6570.

3 Ismail AA, Bahnemann DW. Photochemical splitting of water for hydrogen production by photocatalysis: a review. *Sol Energy Mater Sol Cells* 2014; **128**: 85–101.

4 Nakata K, Fujishima A. TiO$_2$ photocatalysis: design and applications. *J Photochem Photobiol C* 2012; **13**: 169–189.

5 Asahi R, Morikawa T, Ohwaki T, Aoki K, Taga Y. Visible-light photocatalysis in nitrogen-doped titanium oxides. *Science* 2001; **293**: 269–271.

6 Dozzi MV, Selli E. Doping TiO$_2$ with p-block elements: effects on photocatalytic activity. *J Photochem Photobiol C* 2013; **14**: 13–28.

7 Hoffmann MR, Martin ST, Choi W, Bahnemann DW. Environmental applications of semiconductor photocatalysis. *Chem Rev* 1995; **95**: 69–96.

8 Wang SB, Pan L, Song JJ, Mi WB, Zou JJ et al. Titanium-defected undoped anatase TiO$_2$ with p-type conductivity, room-temperature ferromagnetism, and remarkable photocatalytic performance. *J Am Chem Soc* 2015; **137**: 2975–2983.

9 Yang KS, Dai Y, Huang BB, Whangbo MH. Density functional characterization of the band edges, the band gap states, and the preferred doping sites of halogen-doped TiO$_2$. *Chem Mater* 2008; **20**: 6528–6534.

10 Ma XC, Dai Y, Huang BB. Origin of the increased photocatalytic performance of TiO$_2$ nanocrystal composed of pure core and heavily nitrogen-doped shell: a theoretical study. *ACS Appl Mater Interfaces* 2014; **6**: 22815–22822.

11 Odobel F, Pellegrin Y. Recent advances in the sensitization of wide-band-gap nanostructured p-type semiconductors. Photovoltaic and photocatalytic applications. *J Phys Chem Lett* 2013; **4**: 2551–2564.

12 Pelaez M, Nolan NT, Pillai SC, Seery MK, Falaras P et al. A review on the visible light active titanium dioxide photocatalysts for environmental applications. *Appl Catal B* 2012; **125**: 331–349.

13 Serpone N, Emeline AV. Semiconductor photocatalysis—past, present, and future outlook. *J Phys Chem Lett* 2012; **3**: 673–677.

14 Ma XC, Dai Y, Guo M, Huang BB. Insights into the role of surface distortion in promoting the separation and transfer of photogenerated carriers in anatase TiO$_2$. *J Phys Chem C* 2013; **117**: 24496–24502.

15 Chen XB, Liu L, Yu PY, Mao SS. Increasing solar absorption for photocatalysis with black hydrogenated titanium dioxide nanocrystals. *Science* 2011; **331**: 746–750.

16 Liu L, Yu PY, Chen XB, Mao SS, Shen DZ. Hydrogenation and disorder in engineered black TiO$_2$. *Phys Rev Lett* 2013; **111**: 065505.

17 Lu JB, Dai Y, Jin H, Huang BB. Effective increasing of optical absorption and energy conversion efficiency of anatase TiO$_2$ nanocrystals by hydrogenation. *Phys Chem Chem Phys* 2011; **13**: 18063–18068.

18 Awazu K, Fujimaki M, Rockstuhl C, Tominaga J, Murakami H et al. A plasmonic photocatalyst consisting of silver nanoparticles embedded in titanium dioxide. *J Am Chem Soc* 2008; **130**: 1676–1680.

19 Wang P, Huang BB, Qin XY, Zhang XY, Dai Y et al. Ag@AgCl: a highly efficient and stable photocatalyst active under visible light. *Angew Chem Int Ed* 2008; **47**: 7931–7933.

20 Li XN, Ju Z, Li F, Huang Y, Xie YM et al. Visible light responsive Bi$_7$Fe$_3$Ti$_3$O$_{21}$ nanoshelf photocatalysts with ferroelectricity and ferromagnetism. *J Mater Chem A* 2014; **2**: 13366–13372.

21 Wang WJ, Huang BB, Ma XC, Wang ZY, Qin XY et al. Efficient separation of photogenerated electron-hole pairs by the combination of a heterolayered structure and internal polar field in pyroelectric BiOIO$_3$ nanoplates. *Chem Eur J* 2013; **19**: 14777–14780.

22 Zhang R, Dai Y, Lou ZZ, Li ZJ, Wang ZY et al. Layered photocatalyst Bi$_2$O$_2$[BO$_2$(OH)] nanosheets with internal polar field enhanced photocatalytic activity. *Cryst Eng Comm* 2014; **16**: 4931–4934.

23 Batzill M. Fundamental aspects of surface engineering of transition metal oxide photocatalysts. *Energy Environ Sci* 2011; **4**: 3275–3286.

24 Xiang QJ, Yu JG, Jaroniec M. Graphene-based semiconductor photocatalysts. *Chem Soc Rev* 2012; **41**: 782–796.

25 Xiang QJ, Yu JG. Graphene-based photocatalysts for hydrogen generation. *J Phys Chem Lett* 2013; **4**: 753–759.

26 Linic S, Christopher P, Ingram DB. Plasmonic-metal nanostructures for efficient conversion of solar to chemical energy. *Nat Mater* 2011; **10**: 911–921.

27 Clavero C. Plasmon-induced hot-electron generation at nanoparticle/metal-oxide interfaces for photovoltaic and photocatalytic devices. *Nat Photon* 2014; **8**: 95–103.

28 Cheng HF, Fuku K, Kuwahara Y, Mori K, Yamashita H. Harnessing single-active plasmonic nanostructures for enhanced photocatalysis under visible light. *J Mater Chem A* 2015; **3**: 5244–5258.

29 Lou ZZ, Wang ZY, Huang BB, Dai Y. Synthesis and activity of plasmonic photocatalysts. *Chem Cat Chem* 2014; **6**: 2456–2476.

30 Zhang XM, Chen YL, Liu RS, Tsai DP. Plasmonic photocatalysis. *Rep Prog Phys* 2013; **76**: 046401.

31 Wang P, Huang BB, Dai Y, Whangbo MH. Plasmonic photocatalysts: harvesting visible light with noble metal nanoparticles. *Phys Chem Chem Phys* 2012; **14**: 9813–9825.

32 Hou WB, Cronin SB. A review of surface plasmon resonance-enhanced photocatalysis. *Adv Funct Mater* 2013; **23**: 1612–1619.

33 Jiang RB, Li BX, Fang CH, Wang JF. Metal/semiconductor hybrid nanostructures for plasmon-enhanced applications. *Adv Mater* 2014; **26**: 5274–5309.

34 Brongersma ML, Halas NJ, Nordlander P. Plasmon-induced hot carrier science and technology. *Nat Nano* 2015; **10**: 25–34.

35 Ma XC, Dai Y, Yu L, Huang BB. Noble-metal-free plasmonic photocatalyst: hydrogen doped semiconductors. *Sci Rep* 2014; **4**: 3986.

36 Wang Z, Yang CY, Lin TQ, Yin H, Chen P et al. H-doped black titania with very high solar absorption and excellent photocatalysis enhanced by localized surface plasmon resonance. *Adv Funct Mater* 2013; **23**: 5444–5450.

37 Zheng ZK, Huang BB, Qin XY, Zhang XY, Dai Y et al. Facile in situ synthesis of visible-light plasmonic photocatalysts M@TiO$_2$ (M = Au, Pt, Ag) and evaluation of their photocatalytic oxidation of benzene to phenol. *J Mater Chem* 2011; **21**: 9079–9087.

38 Yang D, Sun YY, Tong ZW, Tian Y, Li YB et al. Synthesis of Ag/TiO$_2$ nanotube heterojunction with improved visible-light photocatalytic performance inspired by bioadhesion. *J Phys Chem C* 2015; **119**: 5827–5835.

39 Wang XT, Liow C, Qi DP, Zhu BW, Leow WR et al. Programmable photo-electrochemical hydrogen evolution based on multi-segmented CdS-Au nanorod arrays. *Adv Mater* 2014; **26**: 3506–3512.

40 Solarska R, Bienkowski K, Zoladek S, Majcher A, Stefaniuk T et al. Enhanced water splitting at thin film tungsten trioxide photoanodes bearing plasmonic gold-polyoxometalate particles. *Angew Chem* 2014; **53**: 14196–14200.

41 Sellappan R, Nielsen MG, González-Posada F, Vesborg PCK, Chorkendorff I *et al.* Effects of plasmon excitation on photocatalytic activity of Ag/TiO2 and Au/TiO2 nanocomposites. *J Catal* 2013; **307**: 214–221.

42 Christopher P, Ingram DB, Linic S. Enhancing photochemical activity of semiconductor nanoparticles with optically active Ag nanostructures: photochemistry mediated by Ag surface plasmons. *J Phys Chem C* 2010; **114**: 9173–9177.

43 Zhang L, Blom DA, Wang H. Au-Cu2O core-shell nanoparticles: a hybrid metal-semiconductor heteronanostructure with geometrically tunable optical properties. *Chem Mater* 2011; **23**: 4587–4598.

44 Yu KF, Tian Y, Tatsuma T. Size effects of gold nanaoparticles on plasmon-induced photocurrents of gold-TiO2 nanocomposites. *Phys Chem Chem Phys* 2006; **8**: 5417–5420.

45 Torimoto T, Horibe H, Kameyama T, Okazaki K, Ikeda S *et al.* Plasmon-enhanced photocatalytic activity of cadmium sulfide nanoparticle immobilized on silica-coated gold particles. *J Phys Chem Lett* 2011; **2**: 2057–2062.

46 Thomann I, Pinaud BA, Chen ZB, Clemens BM, Jaramillo TF *et al.* Plasmon enhanced solar-to-fuel energy conversion. *Nano Lett* 2011; **11**: 3440–3446.

47 Shi XW, Ji YL, Hou S, Liu WQ, Zhang H *et al.* Plasmon enhancement effect in Au gold nanorods@Cu2O core-shell nanostructures and their use in probing defect states. *Langmuir* 2015; **31**: 1537–1546.

48 Seh ZW, Liu SH, Low M, Zhang SY, Liu ZL *et al.* Janus Au-TiO2 photocatalysts with strong localization of plasmonic near-fields for efficient visible-light hydrogen generation. *Adv Mater* 2012; **24**: 2310–2314.

49 Ren ST, Wang BY, Zhang H, Ding P, Wang Q. Sandwiched ZnO@Au@Cu2O nanorod films as efficient visible-light-driven plasmonic photocatalysts. *ACS Appl Mater Interfaces* 2015; **7**: 4066–4074.

50 Ma X, Zhao K, Tang HJ, Chen Y, Lu CG *et al.* New insight into the role of gold nanoparticles in Au@CdS core-shell nanostructures for hydrogen evolution. *Small* 2014; **10**: 4664–4670.

51 Mubeen S, Lee J, Singh N, Krämer S, Stucky GD *et al.* An autonomous photosynthetic device in which all charge carriers derive from surface plasmons. *Nat Nano* 2013; **8**: 247–251.

52 Long R, Prezhdo OV. Instantaneous generation of charge-separated state on TiO2 surface sensitized with plasmonic nanoparticles. *J Am Chem Soc* 2014; **136**: 4343–4354.

53 Liu LQ, Ouyang SX, Ye JH. Gold-nanorod-photosensitized titanium dioxide with wide-range visible-light harvesting based on localized surface plasmon resonance. *Angew Chem Int Ed* 2013; **52**: 6689–6693.

54 Fan XF, Zheng WT, Singh DJ. Light scattering and surface plasmons on small spherical particles. *Light Sci Appl* 2014; **3**: e179.

55 Kelly KL, Coronado E, Zhao LL, Schatz GC. The optical properties of metal nanoparticles: the influence of size, shape, and dielectric environment. *J Phys Chem B* 2002; **107**: 668–677.

56 Wang CL, Astruc D. Nanogold plasmonic photocatalysis for organic synthesis and clean energy conversion. *Chem Soc Rev* 2014; **43**: 7188–7216.

57 Evanoff DD, Chumanov G. Synthesis and optical properties of silver nanoparticles and arrays. *Chem Phys Chem* 2005; **6**: 1221–1231.

58 Ma XC, Dai Y, Yu L, Lou ZZ, Huang BB *et al.* Electron-hole pair generation of the visible-light plasmonic photocatalyst Ag@AgCl: enhanced optical transitions involving midgap defect states of AgCl. *J Phys Chem C* 2014; **118**: 12133–12140.

59 Burda C, Chen XB, Narayanan R, El-Sayed MA. Chemistry and properties of nanocrystals of different shapes. *Chem Rev* 2005; **105**: 1025–1102.

60 Mahmoud MA, Chamanzar M, Adibi A, El-Sayed MA. Effect of the dielectric constant of the surrounding medium and the substrate on the surface plasmon resonance spectrum and sensitivity factors of highly symmetric systems: silver nanocubes. *J Am Chem Soc* 2012; **134**: 6434–6442.

61 Hovel H, Fritz S, Hilger A, Kreibig U, Vollmer M. Width of cluster plasmon resonances: bulk dielectric functions and chemical interface damping. *Phys Rev B* 1993; **48**: 18178–18188.

62 Endriz JG, Spicer WE. Surface-plasmon-one-electron decay and its observation in photoemission. *Phys Rev Lett* 1970; **24**: 64–68.

63 Lehmann J, Merschdorf M, Pfeiffer W, Thon A, Voll S *et al.* Surface plasmon dynamics in silver nanoparticles studied by femtosecond time-resolved photoemission. *Phys Rev Lett* 2000; **85**: 2921–2924.

64 Hodak JH, Martini I, Hartland GV. Spectroscopy and dynamics of nanometer-sized noble metal particles. *J Phys Chem B* 1998; **102**: 6958–6967.

65 Liu ZW, Hou WB, Pavaskar P, Aykol M, Cronin SB. Plasmon resonant enhancement of photocatalytic water splitting under visible illumination. *Nano Lett* 2011; **11**: 1111–1116.

66 Manjavacas A, Liu JG, Kulkarni V, Nordlander P. Plasmon-induced hot carriers in metallic nanoparticles. *ACS Nano* 2014; **8**: 7630–7638.

67 Mubeen S, Hernandez-Sosa G, Moses D, Lee J, Moskovits M. Plasmonic photosensitization of a wide band gap semiconductor: converting plasmons to charge carriers. *Nano Lett* 2011; **11**: 5548–5552.

68 Grätzel M. Photoelectrochemical cells. *Nature* 2001; **414**: 338–344.

69 Hashimoto K, Irie H, Fujishima A. TiO2 photocatalysis: a historical overview and future prospects. *Jpn J Appl Phys* 2005; **44**: 8269.

70 Sundararaman R, Narang P, Jermyn AS, Goddard III WA, Atwater HA. Theoretical predictions for hot-carrier generation from surface plasmon decay. *Nat Commun* 2014; **5**: 5788.

71 Bernardi M, Mustafa J, Neaton JB, Louie SG. Theory and computation of hot carriers generated by surface plasmon polaritons in noble metals. *Nat Commun* 2015; **6**: 7044.

72 Zhao GL, Kozuka H, Yoko T. Sol-gel preparation and photoelectrochemical properties of TiO2 films containing Au and Ag metal particles. *Thin Solid Films* 1996; **277**: 147–154.

73 Ohko Y, Tatsuma T, Fujii T, Naoi K, Niwa C *et al.* Multicolour photochromism of TiO2 films loaded with silver nanoparticles. *Nat Mater* 2003; **2**: 29–31.

74 Furube A, Du LC, Hara K, Katoh R, Tachiya M. Ultrafast plasmon-induced electron transfer from gold nanodots into TiO2 nanoparticles. *J Am Chem Soc* 2007; **129**: 14852–14853.

75 Asbury JB, Hao EC, Wang YQ, Ghosh HN, Lian TQ. Ultrafast electron transfer dynamics from molecular adsorbates to semiconductor nanocrystalline thin films. *J Phys Chem B* 2001; **105**: 4545–4557.

76 DuChene JS, Sweeny BC, Johnston-Peck AC, Su D, Stach EA *et al.* Prolonged hot electron dynamics in plasmonic-metal/semiconductor heterostructures with implications for solar photocatalysis. *Angew Chem Int Ed* 2014; **53**: 7887–7891.

77 Liu LQ, Li P, Wang T, Hu HL, Jiang HY *et al.* Constructing a multicomponent junction for improved visible-light photocatalytic performance induced by Au nanoparticles. *Chem Commun* 2015; **51**: 2173–2176.

78 Ha JW, Ruberu TPA, Han R, Dong B, Vela J *et al.* Super-resolution mapping of photogenerated electron and hole separation in single metal-semiconductor nanocatalysts. *J Am Chem Soc* 2014; **136**: 1398–1408.

79 Li A, Zhang P, Chang XX, Cai WT, Wang T *et al.* Gold nanorod@TiO2 yolk-shell nanostructures for visible-light-driven photocatalytic oxidation of benzyl alcohol. *Small* 2015; **11**: 1892–1899.

80 Tung RT. The physics and chemistry of the Schottky barrier height. *Appl Phys Rev* 2014; **1**: 011304.

81 Park JY, Kim SM, Lee H, Naik B. Hot electron and surface plasmon-driven catalytic reaction in metal-semiconductor nanostructures. *Catal Lett* 2014; **144**: 1996–2004.

82 Watanabe A, Kozuka H. Photoanodic properties of sol-gel-derived Fe2O3 thin films containing dispersed gold and silver particles. *J Phys Chem B* 2003; **107**: 12713–12720.

83 Giugni A, Torre B, Toma A, Francardi M, Malerba M *et al.* Hot-electron nanoscopy using adiabatic compression of surface plasmons. *Nat Nano* 2013; **8**: 845–852.

84 Li JT, Cushing SK, Zheng P, Meng FK, Chu D *et al.* Plasmon-induced photonic and energy-transfer enhancement of solar water splitting by a hematite nanorod array. *Nat Commun* 2013; **4**: 2651.

85 Knight MW, Sobhani H, Nordlander P, Halas NJ. Photodetection with active optical antennas. *Science* 2011; **332**: 702–704.

86 Knight MW, Wang Y, Urban AS, Sobhani A, Zheng BY *et al.* Embedding plasmonic nanostructure diodes enhances hot electron emission. *Nano Lett* 2013; **13**: 1687–1692.

87 Fang CH, Jia HL, Chang S, Ruan QF, Wang P *et al.* (Gold core)/(titania shell) nanostructures for plasmon-enhanced photon harvesting and generation of reactive oxygen species. *Energy Environ Sci* 2014; **7**: 3431–3438.

88 Li BX, Gu T, Ming T, Wang JX, Wang P *et al.* (Gold core)@(ceria shell) nanostructures for plasmon-enhanced catalytic reactions under visible light. *ACS Nano* 2014; **8**: 8152–8162.

89 Liu LQ, Dao TD, Kodiyath R, Kang Q, Abe H *et al.* Plasmonic Janus-composite photocatalyst comprising Au and C-TiO2 for enhanced aerobic oxidation over a broad visible-light range. *Adv Funct Mater* 2014; **24**: 7754–7762.

90 Fan XM, Xu CX, Hao XL, Tian ZS, Lin Y. Synthesis and optical properties of Janus structural ZnO/Au nanocomposites. *EPL* 2014; **106**: 67001.

91 Ma XC, Dai Y, Yu L, Huang BB. New basic insights into the low hot electron injection efficiency of gold-nanoparticle-photosensitized titanium dioxide. *ACS Appl Mater Interfaces* 2014; **6**: 12388–12394.

92 Li JT, Cushing SK, Zheng P, Senty T, Meng FK *et al.* Solar hydrogen generation by a CdS-Au-TiO2 sandwich nanorod array enhanced with Au nanoparticle as electron relay and plasmonic photosensitizer. *J Am Chem Soc* 2014; **136**: 8438–8449.

93 Mrovec M, Albina JM, Meyer B, Elsässer C. Schottky barriers at transition-metal/SrTiO3 (001) interfaces. *Phys Rev B* 2009; **79**: 245121.

94 Rao FY, Kim M, Freeman AJ, Tang SP, Anthony M. Structural and electronic properties of transition-metal/BaTiO3 (001) interfaces. *Phys Rev B* 1997; **55**: 13953–13960.

95 Tamura T, Ishibashi S, Terakura K, Weng HM. First-principles study of the rectifying properties of Pt/TiO2 interface. *Phys Rev B* 2009; **80**: 195302.

96 Smith JG, Faucheaux JA, Jain PK. Plasmon resonances for solar energy harvesting: a mechanistic outlook. *Nano Today* 2015; **10**: 67–80.

97 Lin ZJ, Wang XH, Liu J, Tian ZY, Dai LC *et al.* On the role of localized surface plasmon resonance in UV-Vis light irradiated Au/TiO2 photocatalysis systems: pros and cons. *Nanoscale* 2015; **7**: 4114–4123.

98 Persson BNJ. Polarizability of small spherical metal particles: influence of the matrix environment. *Surf Sci* 1993; **281**: 153–162.

99 Bosbach J, Hendrich C, Stietz F, Vartanyan T, Träger F. Ultrafast dephasing of surface plasmon excitation in silver nanoparticles: influence of particle size, shape, and chemical surrounding. *Phys Rev Lett* 2002; **89**: 257404.

100 Petek H, Weida MJ, Nagano H, Ogawa S. Real-time observation of adsorbate atom motion above a metal surface. *Science* 2000; **288**: 1402–1404.

101 Jain PK, Qian W, El-Sayed MA. Ultrafast cooling of photoexcited electrons in gold nanoparticle−thiolated DNA conjugates involves the dissociation of the gold−thiol bond. *J Am Chem Soc* 2006; **128**: 2426–2433.

102 Kale MJ, Avanesian T, Xin HL, Yan J, Christopher P. Controlling catalytic selectivity on metal nanoparticles by direct photoexcitation of adsorbate-metal bonds. *Nano Lett* 2014; **14**: 5405–5412.

103 Kale MJ, Avanesian T, Christopher P. Direct photocatalysis by plasmonic nanostructures. *ACS Catal* 2014; **4**: 116–128.

104 Cushing SK, Li JT, Meng FK, Senty TR, Suri S *et al*. Photocatalytic activity enhanced by plasmonic resonant energy transfer from metal to semiconductor. *J Am Chem Soc* 2012; **134**: 15033–15041.

105 Sahoo H. Forster resonance energy transfer – a spectroscopic nanoruler: principle and applications. *J Photochem Photobiol C* 2011; **12**: 20–30.

106 Dressel M, Grüner G. *Electrodynamics of solids: optical properties of electrons in matter*. Cambridge: Cambridge University Press; 2002.

107 Liu TX, Li BX, Hao YG, Han F, Zhang LL *et al*. A general method to diverse silver/mesoporous-metal-oxide nanocomposites with plasmon-enhanced photocatalytic activity. *Appl Catal B* 2015; **165**: 378–388.

108 Meng FK, Cushing SK, Li JT, Hao SM, Wu NQ. Enhancement of solar hydrogen generation by synergistic interaction of La$_2$Ti$_2$O$_7$ photocatalyst with plasmonic gold nanoparticles and reduced graphene oxide nanosheets. *ACS Catal* 2015; **5**: 1949–1955.

109 Near RD, Hayden SC, El-Sayed MA. Thin to thick, short to long: spectral properties of gold nanorods by theoretical modeling. *J Phys Chem C* 2013; **117**: 18653–18656.

110 Mahmoud MA, El-Sayed MA. Different plasmon sensing behavior of silver and gold nanorods. *J Phys Chem Lett* 2013; **4**: 1541–1545.

111 Chen HJ, Shao L, Li Q, Wang JF. Gold nanorods and their plasmonic properties. *Chem Soc Rev* 2013; **42**: 2679–2724.

112 Seh ZW, Liu SH, Zhang SY, Bharathi MS, Ramanarayan H *et al*. Anisotropic growth of titania onto various gold nanostructures: synthesis, theoretical understanding, and optimization for catalysis. *Angew Chem Int Ed* 2011; **50**: 10140–10143.

113 Kumar MK, Krishnamoorthy S, Tan LK, Chiam SY, Tripathy S *et al*. Field effects in plasmonic photocatalyst by precise SiO$_2$ thickness control using atomic layer deposition. *ACS Catal* 2011; **1**: 300–308.

114 Ingram DB, Christopher P, Bauer JL, Linic S. Predictive model for the design of plasmonic metal/semiconductor composite photocatalysts. *ACS Catal* 2011; **1**: 1441–1447.

115 Mohamed MB, Volkov V, Link S, El-Sayed MA. The 'lightning' gold nanorods: fluorescence enhancement of over a million compared to the gold metal. *Chem Phys Lett* 2000; **317**: 517–523.

116 Dulkeith E, Niedereichholz T, Klar TA, Feldmann J, von Plessen G *et al*. Plasmon emission in photoexcited gold nanoparticles. *Phys Rev B* 2004; **70**: 205424.

117 Ingram DB, Linic S. Water splitting on composite plasmonic-metal/semiconductor photoelectrodes: evidence for selective plasmon-induced formation of charge carriers near the semiconductor surface. *J Am Chem Soc* 2011; **133**: 5202–5205.

118 Atwater HA, Polman A. Plasmonics for improved photovoltaic devices. *Nat Mater* 2010; **9**: 205–213.

119 Govorov AO, Zhang H. Kinetic density functional theory for plasmonic nanostructures: breaking of the plasmon peak in the quantum regime and generation of hot electrons. *J Phys Chem C* 2015; **119**: 6181–6194.

120 Govorov AO, Zhang H, Demir HV, Gun'ko YK. Photogeneration of hot plasmonic electrons with metal nanocrystals: quantum description and potential applications. *Nano Today* 2014; **9**: 85–101.

121 Govorov AO, Zhang H, Gun'ko YK. Theory of photoinjection of hot plasmonic carriers from metal nanostructures into semiconductors and surface molecules. *J Phys Chem C* 2013; **117**: 16616–16631.

122 Zhang H, Govorov AO. Optical generation of hot plasmonic carriers in metal nanocrystals: the effects of shape and field enhancement. *J Phys Chem C* 2014; **118**: 7606–7614.